THE PERFORMANCE OF NASA RESEARCH HYDROGEN MASERS

Victor S. Reinhardt
Goddard Space Flight Center

Lauren J. Rueger
The Johns Hopkins University
Applied Physics Laboratory

ABSTRACT

The Johns Hopkins University (JHU), Applied Physics Laboratory (APL), under contract to NASA/ Goddard Space Flight Center, is engineering a new generation of field operable hydrogen masers (NR) based on prior NASA NP and NX designs. These units incorporate improvements in magnetic shielding, lower noise electronics, better thermal control and have a microprocessor for operation, monitoring and diagnostic functions. They are ruggedly built for transportability and ease of service anywhere in the world.

INTRODUCTION

NASA has planned experiments in the coming years that will require reference frequency sources of better than 10^{-14} $\Delta f/f$ for 1000 second averaging times to be available at remote sites throughout the world. The NR masers are being designed to meet this need and to provide monitoring functions to assure that the reference frequency is valid during experiments. This paper is a status or progress report on the development program.

NR Design Improvements

The NR masers have major design improvements as compared with past designs. A major breakthrough in terms of field serviceability is field interchangeable vacuum pumps. Hydrogen consumption in the NR masers has been reduced to allow the maser's Vacion pumps to be connected to the maser through a series of 1½ inch (3.81 cm) O.D. vacuum line valves. This enables the vacuum pumps to be replaced in the field without letting the maser up to air. Dry runs have shown that a pump can be replaced and the maser put back in operation in about 2 hours. Only a small fore pump to pump out the replacement Vacion pump is needed to do this.

The NR design has improved magnetic shielding. There are four concentric shells of molypermalloy 0.050″ (0.13 cm) thick shields spaced about ¾ inch (1.9 cm) apart. The Vacion pumps have individual molypermalloy shields, and the source assembly is shielded with the same weight stock.

The thermal time constant of the resonant cavity has been increased about tenfold by mounting it on delrin plastic standoffs and reducing the size of the escape openings of the radiation shields.

The frame and all constant temperature surfaces have been made of heavy gauge aluminum to reduce thermal gradients. The power supplies have been isolated and remotely placed in the rear of the cabinet to minimize local hot spots.

One of the shipping problems with the NP and NX masers was the reluctance of air carriers to take a device with a high-pressure hydrogen gas bottle on board. The NR has eliminated this problem by a low pressure electrolysis system for its hydrogen supply.

The JHU/APL experience in low noise electronics was used to provide new multipliers, I.F. amplifiers, and mixers for the NR design.

The magnetic field currents in the main solenoid and neck coil were put under a part in a million regulations and are now independent of any primary supply voltage variation.

A number of circuits in the NP and NX designs that are in the VCO control loop were not in temperature-controlled compartments. The NR design has placed the following circuits in a new temperature-controlled compartment, the VCO, the autotune reference oscillator, the autotune

reference oscillator, the autotune multipliers, the 5.7 kHz synthesizer, the 5 MHz isolation buffers, the magnetic current regulator, and the cavity control 18 bit D/A converter.

The 5.7 kHz synthesizer is based on a very reliable design qualified for space service on another APL program. It is a three-stage cascaded divide and mix system that provides a frequency resolution of 10^{-17} at the maser frequency.

Recent maser application experiences have indicated the requirement for good buffer isolation. A new buffer design has been provided that realizes 120 dB of output to input isolation.

A microprocessor, the Intersil IM 6100, provides in software many functions formerly done by discrete logic. A clock system provides two separate one pulse per second outputs that are each adjustable in epoch. An autotuner function automatically tunes the maser from either an internal crystal reference or an external reference oscillator. Sensors are provided to measure voltages, currents, and temperatures, as well as switch positions; these are converted to digital form for recording purposes. The microprocessor can also interface on any of three RS/232-C communications interfaces.

There has been a high degree of parts and subsystem interchangeability provided. It takes only a few minutes to change any major electronic package.

Maser Block Diagram

In figure 1 is shown a block diagram of the NR maser. The maser has its own thermal servos, the inner cavity is a thermally tuned aluminum cylinder that is held about 2°C above the outer oven temperature. The receiver is in a separately thermal-controlled box adjacent to the top of the maser cavity. It includes 5 MHz to 0.4 MHz; 20 MHz; and 1400 MHz frequency synthesizers and the 5.7 kHz phase detector. The new temperature controlled box contains the VCO, buffers, reference oscillator, autotuner multipliers and mixer, the 18 bit D/A converter to control the cavity, and the magnetic regulator with controls. The microprocessor is not temperature controlled. It contains the clock, the keyboard, the display of five lines of 20 characters each, the alarm, and the external interface circuits for teletype and recorder. The vacuum electronics, gas pressure controls, and power system are not shown on the diagram.

Hardware Detailed Design

In figure 2 is shown the basic design of NASA masers. Hydrogen is introduced into the source bulb where it is dissociated and leaves through the collimator. A variable field quadrupole electromagnet selects the atoms of the appropriate energy, and a mechanical beam shutter is used to modulate the beam flux. The quartz storage bulb is elongated in this design and the inner surface coated with Teflon. The resonant cavity has movable end plates for coarse frequency adjustment and is thermally controlled for fine frequency adjustment. The cavity is magnetically shielded and multistage temperature controlled.

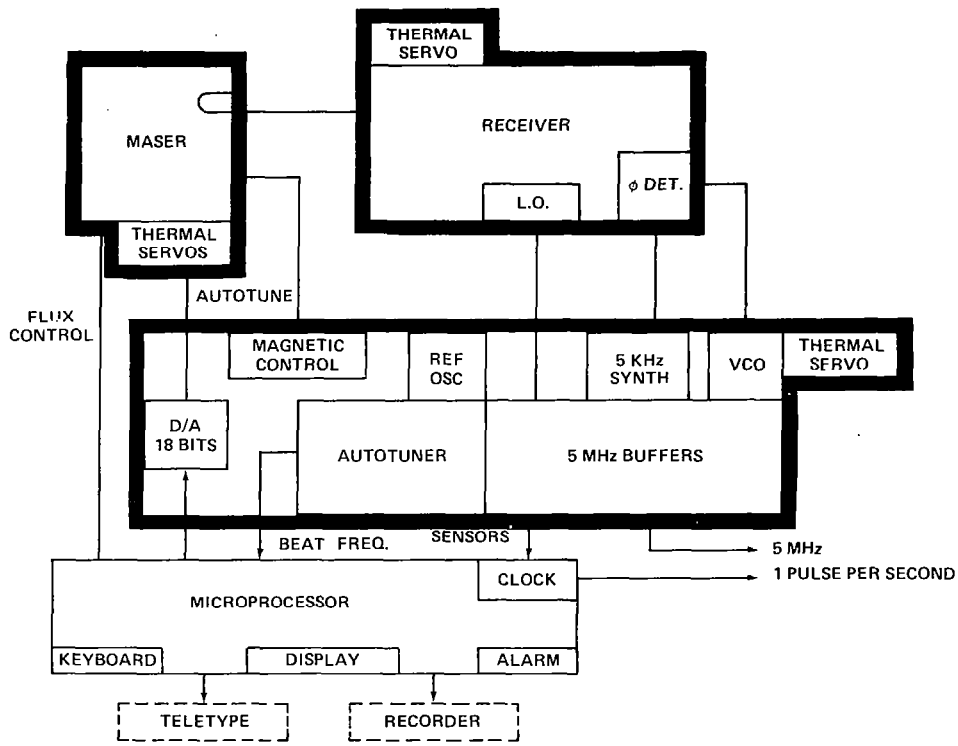

Figure 1. NR maser block diagram.

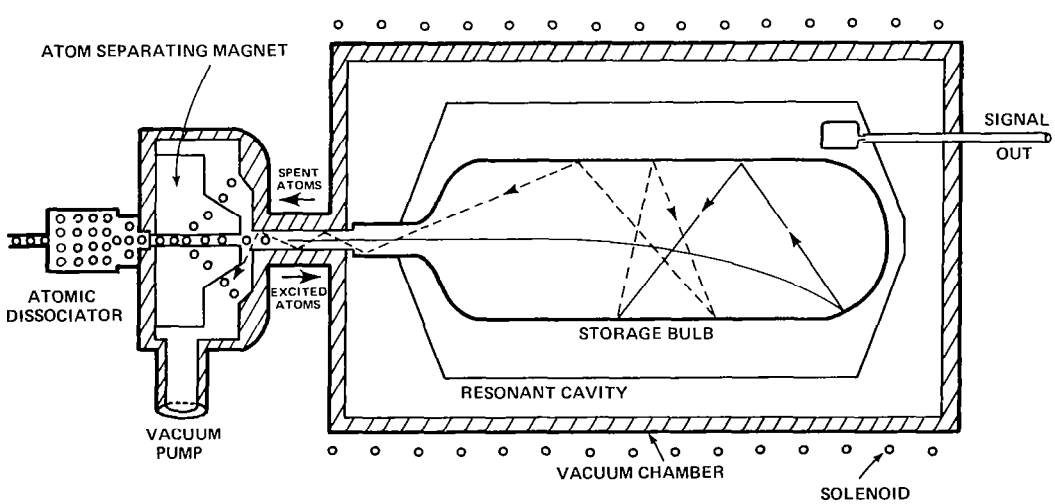

Figure 2. Principal elements of the NASA hydrogen maser.

In figure 3 is shown the Vacion pumping system of the maser. Notice there are two Vacion pumps. One pumps the storage bulb and source region, and the other pumps the bell jar and microwave cavity region. The dual pumping system is used to reduce contamination of the storage bulb from materials outgassed by the bell jar or cavity. The system is designed so all O-rings exposed to the ambient air pumped by the bell jar system except for one O-ring which seals the source dissociator bulb to the source region.

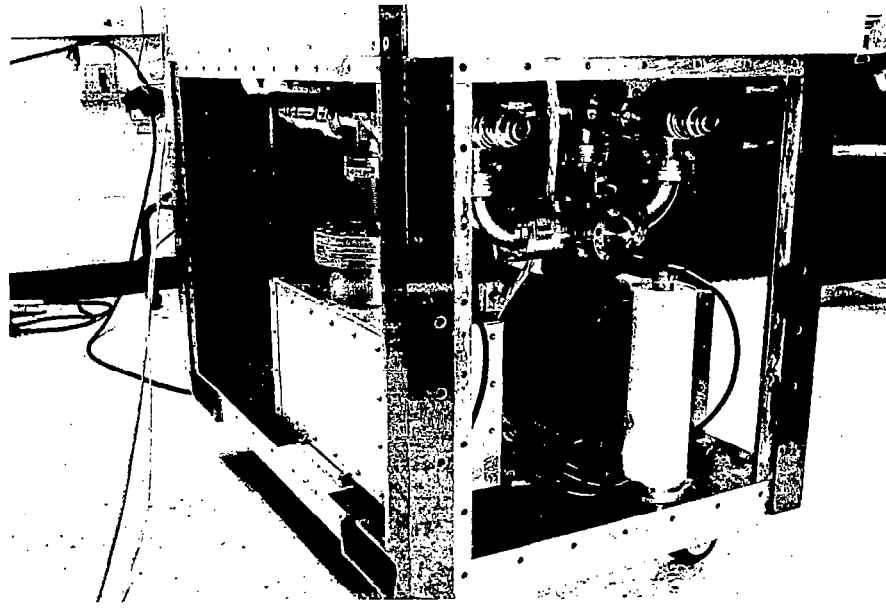

Figure 3. NR maser pumping system.

In figure 4 is shown the new hydrogen generators. Application of 1.5 volts at 2 milliamperes provides hydrogen by electrolysis of a water solution of potassium hydroxide. The negative electrode has a palladium film that provides spectroscopically pure hydrogen flow at room temperature.

In figure 5 is shown the source assembly; the electromagnets, the mechanical shutter, the two-stage vacuum system, one pumping on the vacuum seals, the other pumping on the spent hydrogen. Fiber optics are provided to observe the color and intensity of the discharge in the source bulb.

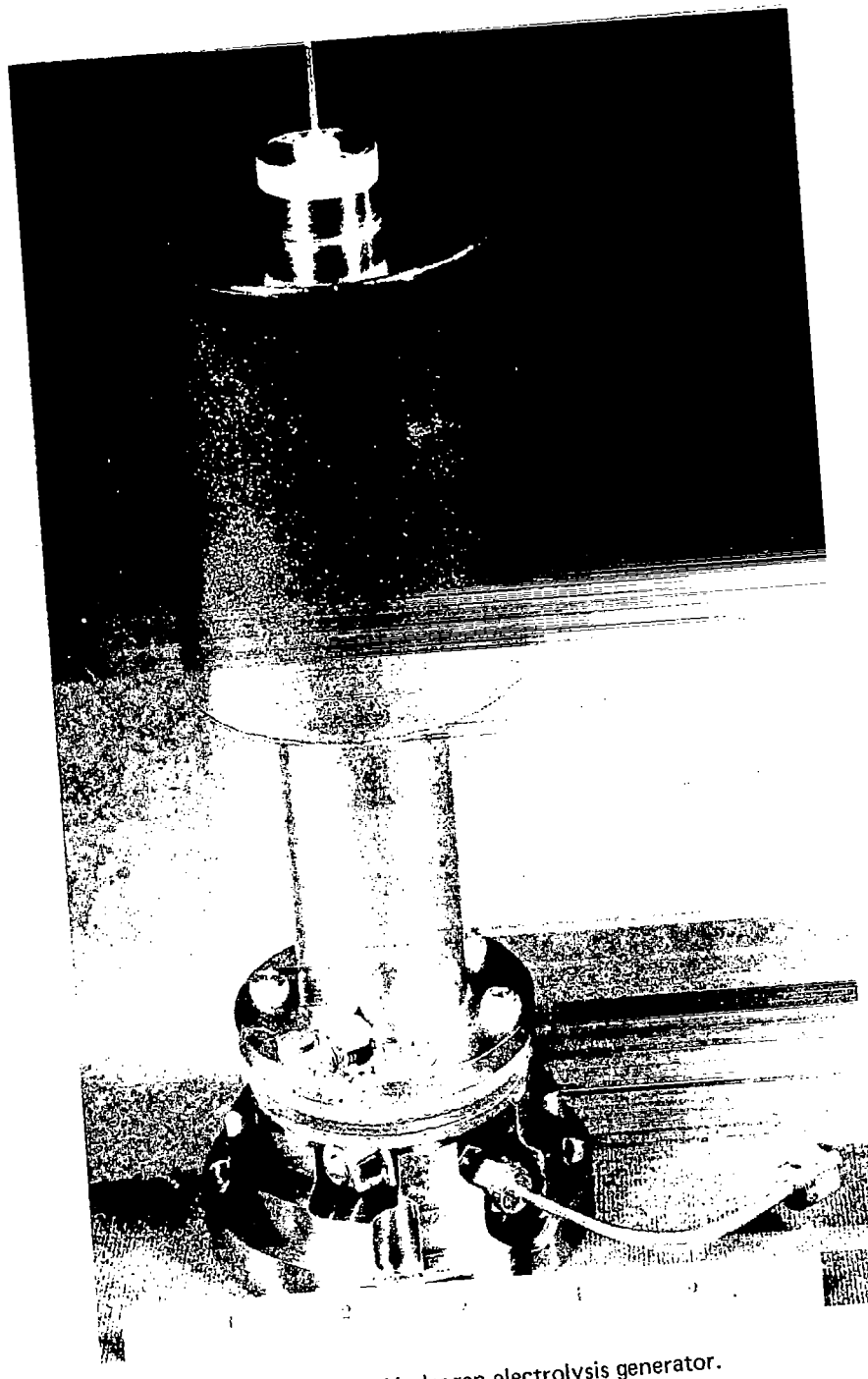

Figure 4. Hydrogen electrolysis generator.

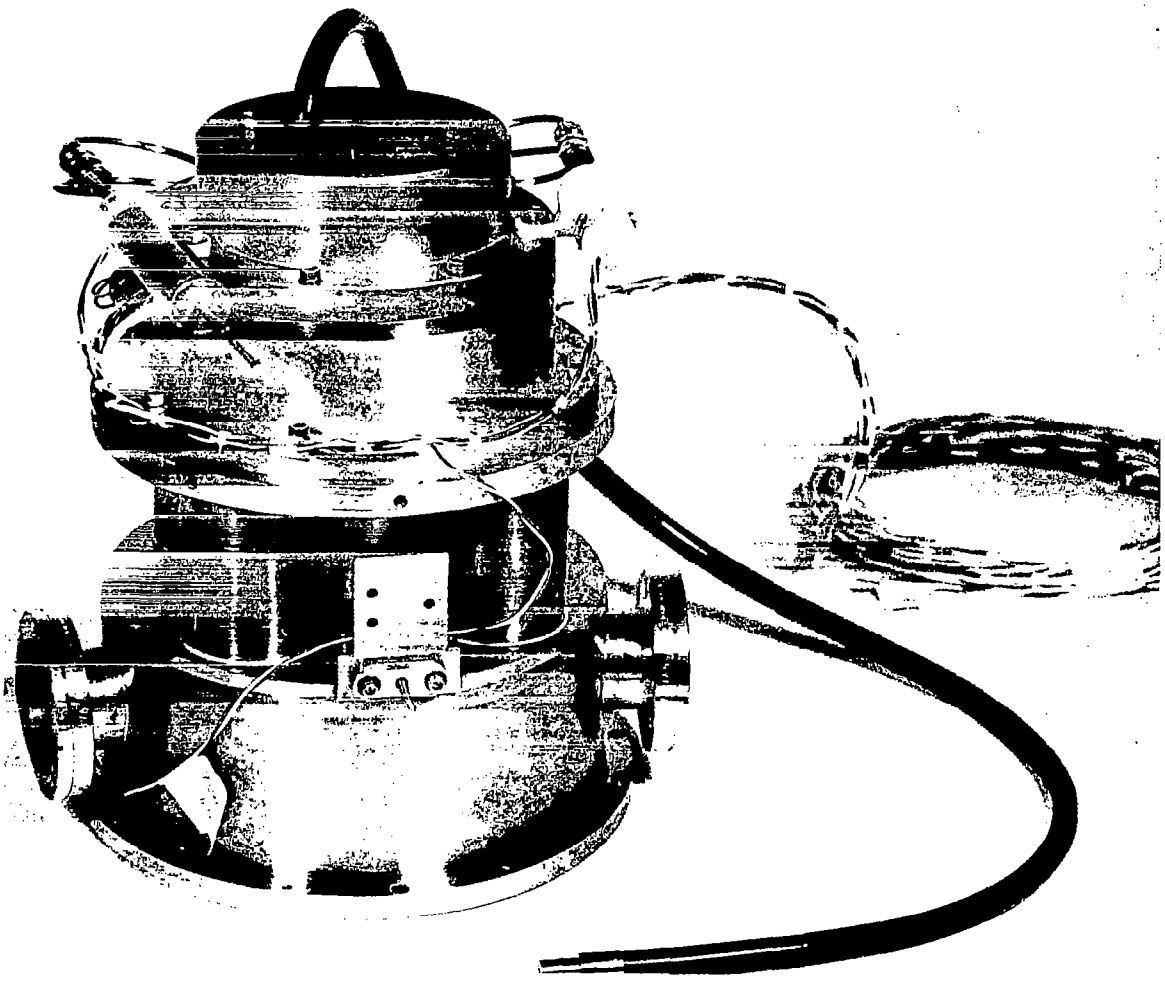

Figure 5. Source assembly.

In figure 6 are shown the various cylinders that make up the physics package. Starting on the left is the primary resonant cavity with heater, Zeeman coil, and thermistors attached by a ceramic cement; two aluminum radiation shields; the vacuum chamber with its heater and thermistor sensors; the solenoid with end trim coils; a magnetic shield, a thermal insulator, a magnetic shield, a thermal insulation; a magnetic shield; and finally, a heavy aluminum constant temperature cylinder.

In figure 7 is shown the base on which these cylinders fit. The lower movable end plate of the resonant cavity can be seen, and the quartz storage bulb is in place.

In figure 8 is shown the front view of the assembled NR maser. All controls except the microprocessor keyboard are enclosed behind doors. The meters indicate vital functions in the maser.

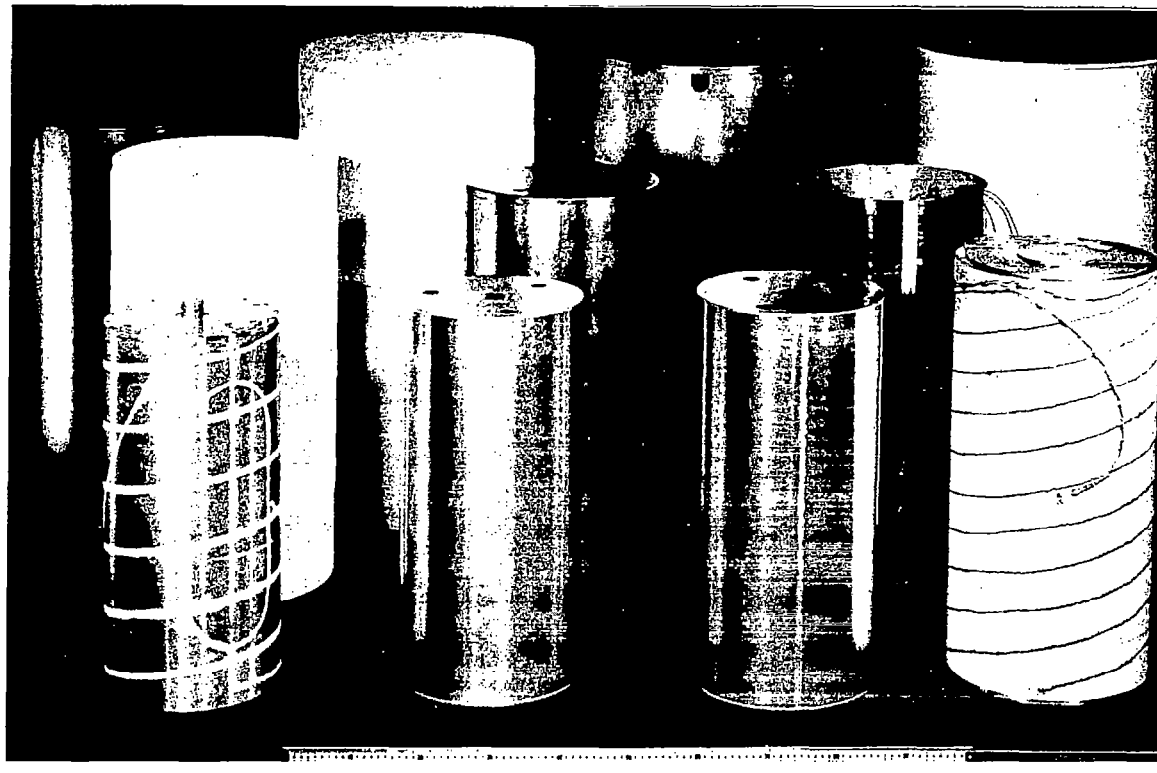

Figure 6. Physics package cylinders.

The lower right meter indicates the I.F. signal level at 5.7 kHz. The lower left meter indicates VCO phase lock. The red jewel at the bottom is a fiber optics indication of the source color and intensity.

In figure 9 is shown the maser opened up to indicate the accessibility of the maser for servicing. On the bottom are fork-lift holes for handling the maser on a loading dock. At the rear are stored four 12-volt batteries for standby power. The vacuum system is made of standard Varian 1½ inch (3.81 cm) O.D. vacuum line assemblies. The rear of the microprocessor is visible; the third thermal control box is shown extended on its rails. On the front are the magnetic field controls; on the bottom are the manual synthesizer controls (the synthesizer can also be under microprocessor control). The caster assemblies are for rolling the maser around on the level and are detachable leaving a package about 22″ (55.8 cm) wide, 38″ (96.5 cm) deep and 62″ (156.5 cm) tall. The rear door carries all of the switching regulator supplies: 120 volts AC to 28 volts DC; 28 ± 5 volts DC to 28 volts DC; 28 volts DC to ±18 volts; and 28 volts DC to +5 volts.

In figure 10 is shown further opening of the microprocessor modules and a panel removed from the third thermal servo box. The Oscilloquartz model B5400 oscillators are visible along the edge, the current regulator circuits are on the hinged lid, the synthesizer boards are visible.

Figure 7. Physics package base with storage bulb.

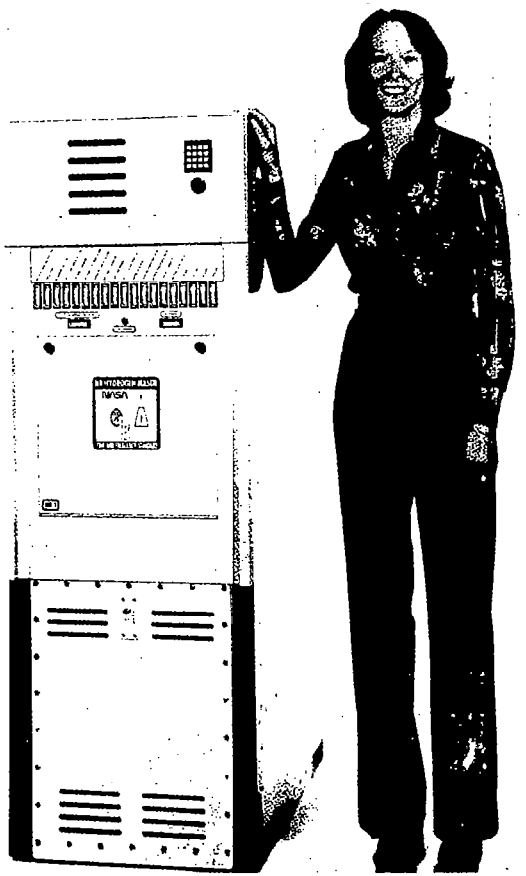

Figure 8. Front view of NR maser.

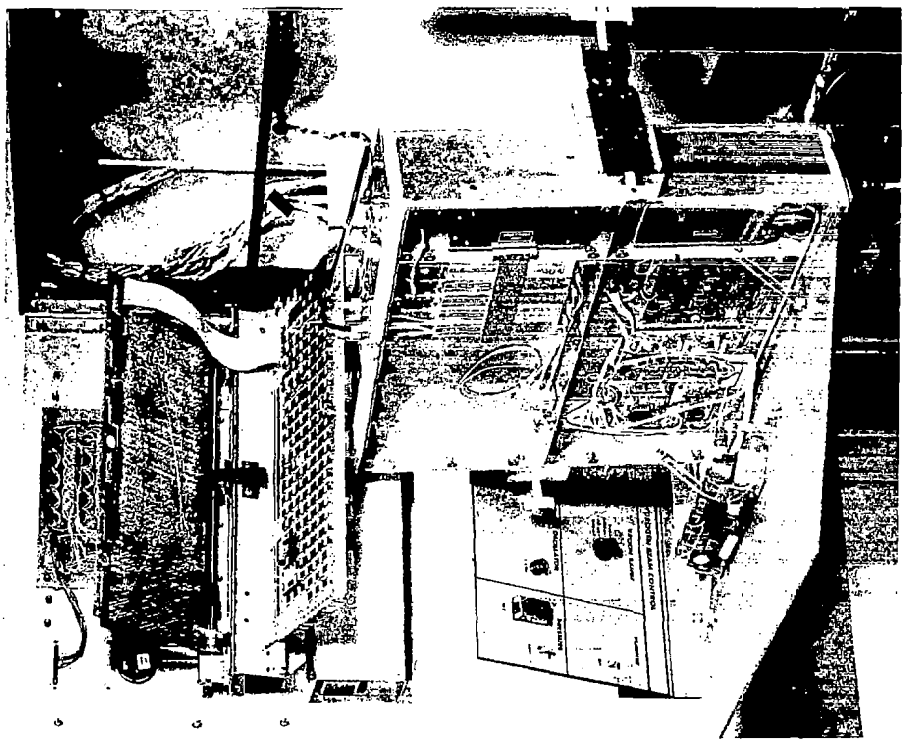

Figure 10. Close-up of NR maser exposed electronics.

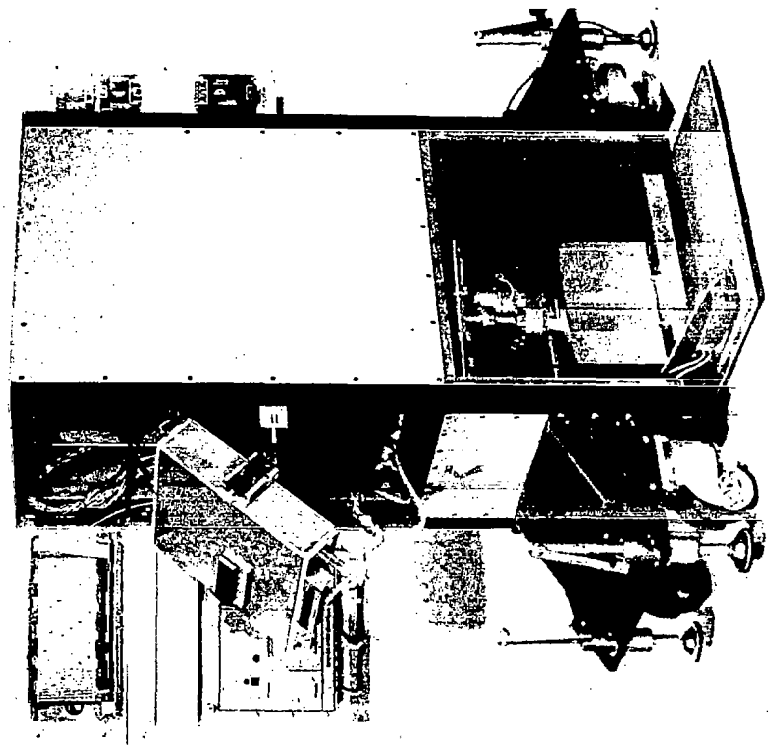

Figure 9. NR maser opened for servicing.

In figure 11 is shown a close-up of a synthesizer board to show how the parts are labeled as in the schematic diagrams, making servicing easy.

In figure 12 is shown the receiver; the multipliers are at the top, the maser signal goes through a low noise preamplifier, a double-balanced image-reject mixer, and the I.F. amplifiers. The overall noise figure is less than 2 dB.

In figure 13 is shown the 200 to 1400 MHz multiplier.

In figure 14 are shown the APL staff working part-time on the maser program who have brought the design to its present status. Clockwise from lower left: C. M. Blackburn, E. E. Mengel, D. W. Stover, P. J. Underwood, A. G. Bates, H. L. Smigocki, L. J. Rueger, L. E. Stillman, and J. R. Norton.

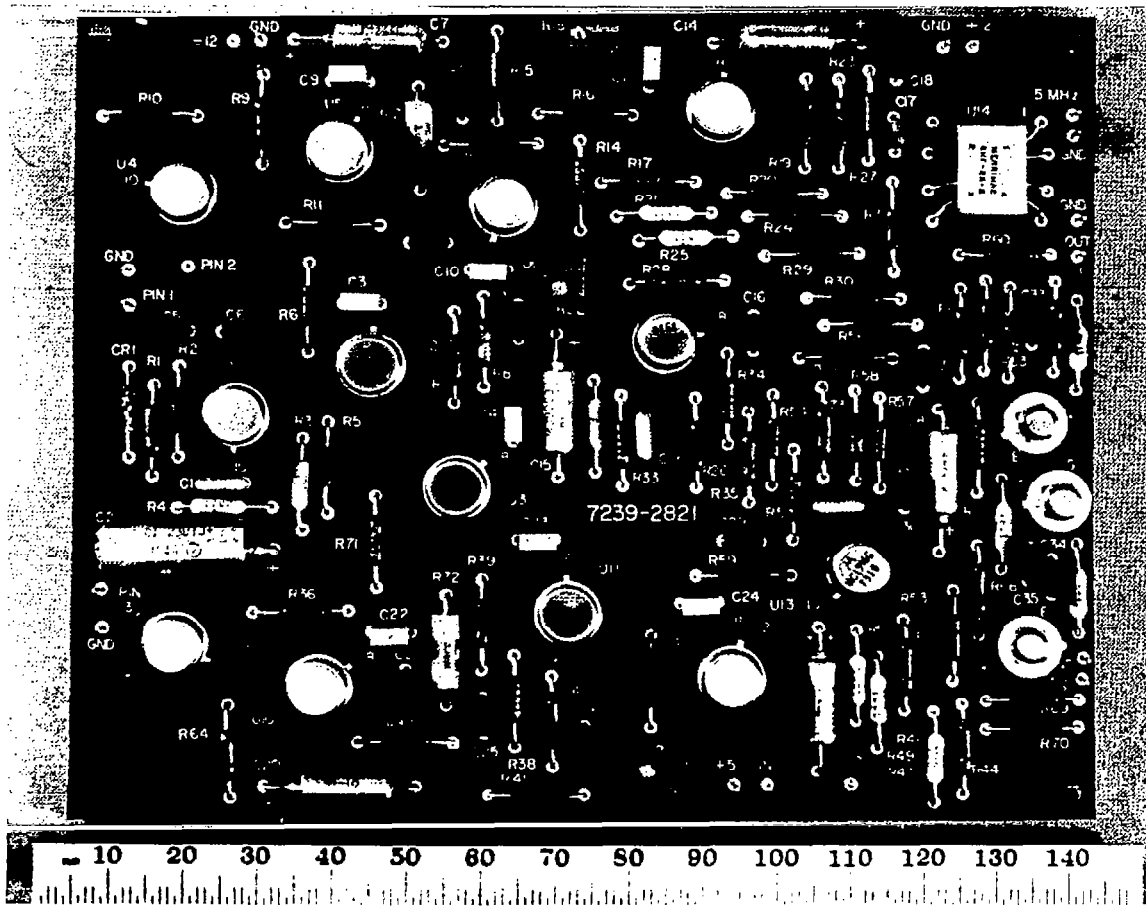

Figure 11. NR maser synthesizer board #2.

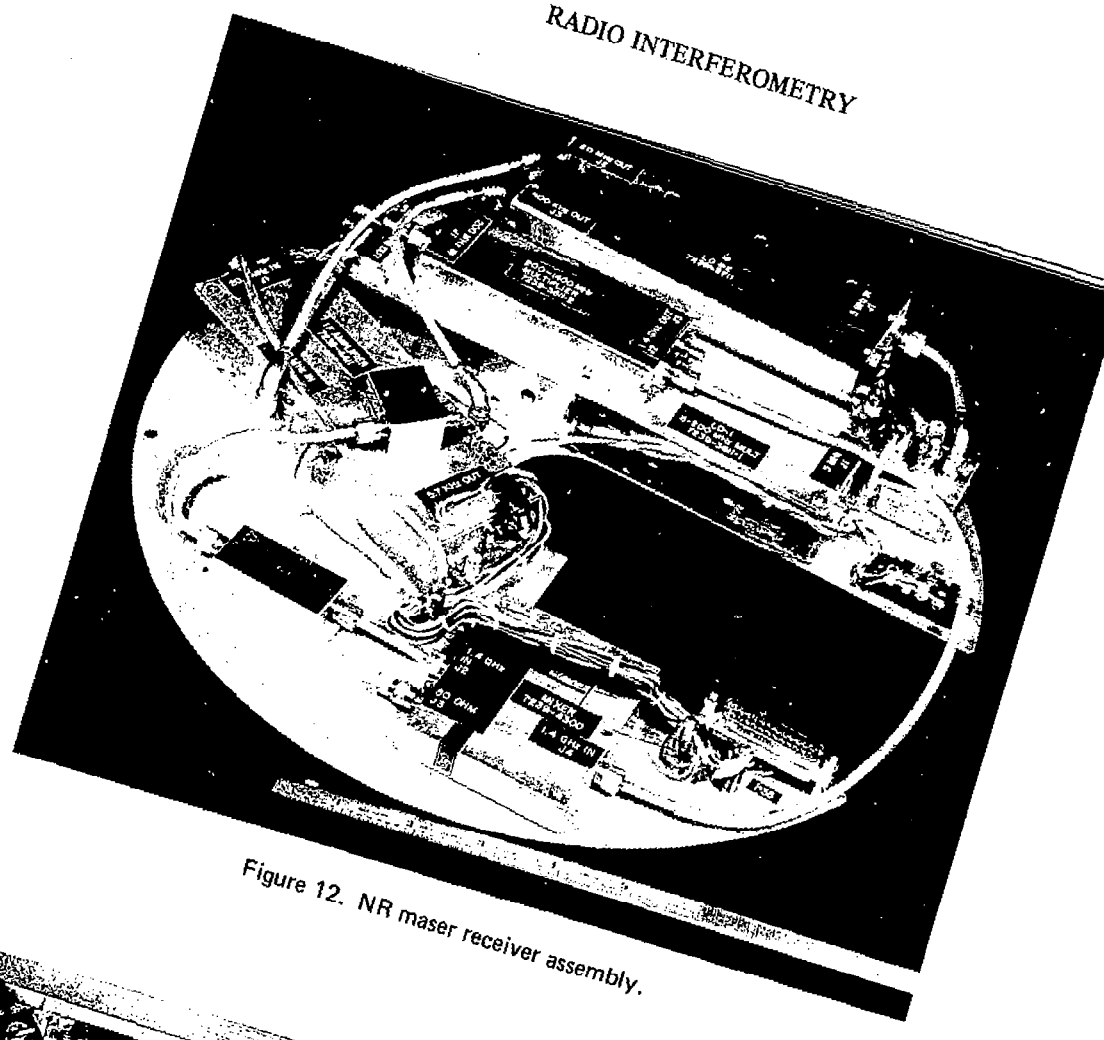

Figure 12. NR maser receiver assembly.

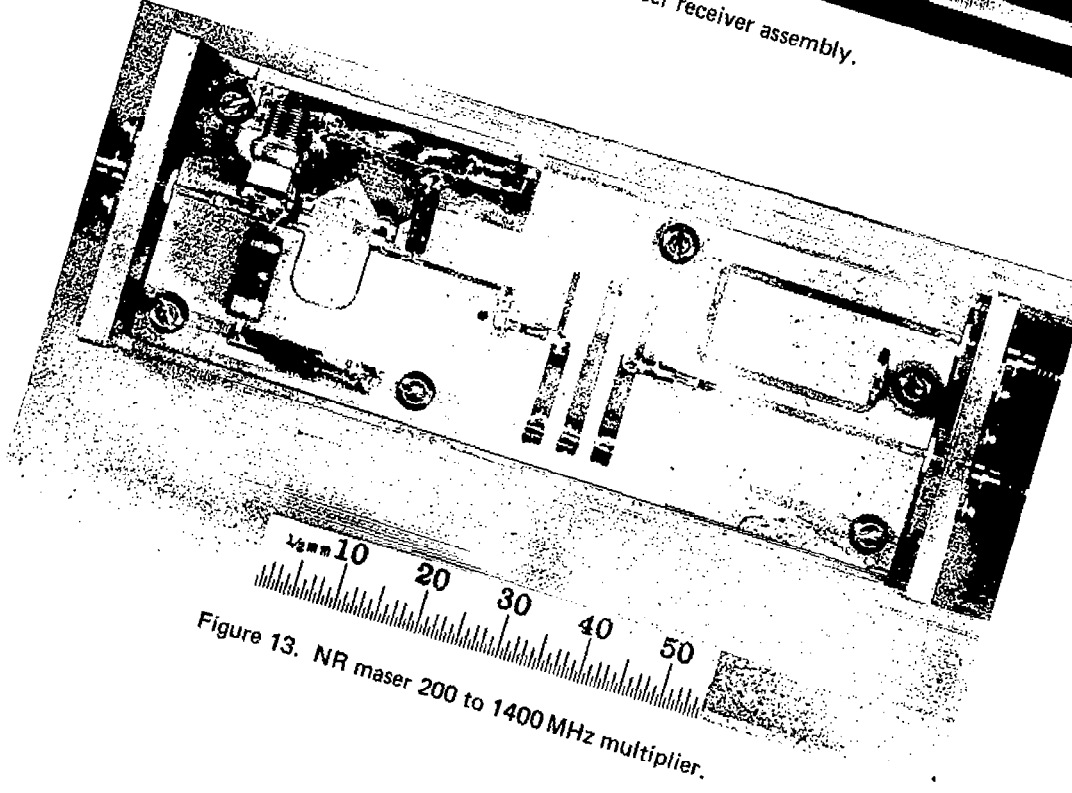

Figure 13. NR maser 200 to 1400 MHz multiplier.

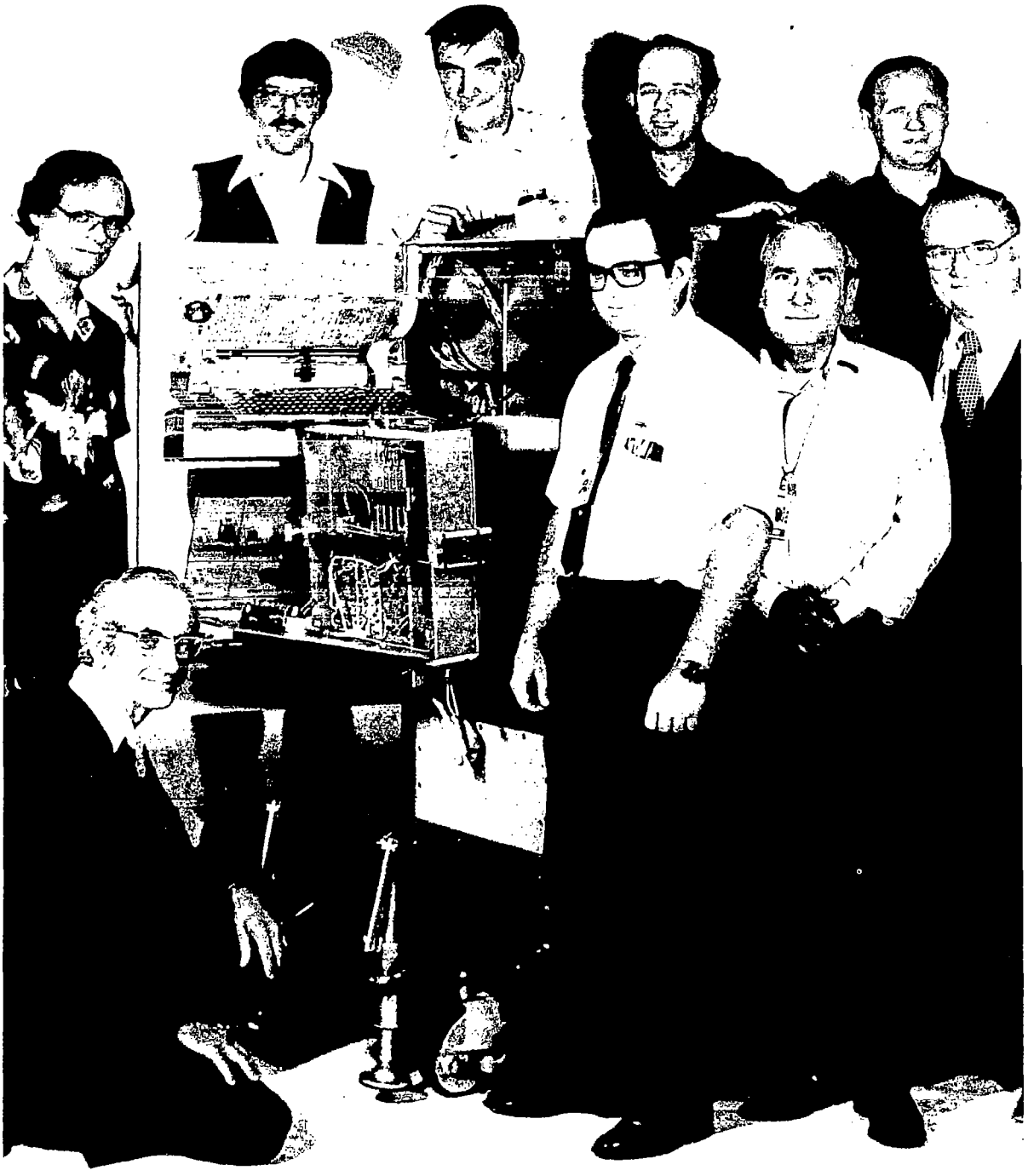

Figure 14. APL staff workers on NR maser.

Results to Date

Line Q. Two NR masers have been constructed and are designated NR-1 and NR-2. The line Q has been measured as 2×10^9.

Pressure Sensitivity. The pressure sensitivity of NR-2 has been measured by placing it in an altitude chamber. The average pressure sensitivity was 5×10^{-15} per inch (2.54 cm) of mercury.

Magnetic Sensitivity. The magnetic susceptibilities of the NR masers were measured by placing the masers in a large solenoid and observing changes in the maser frequency output against a reference maser. The standard procedure was to switch the solenoid field between plus and minus 0.5 gauss and to observe the difference in the maser frequency output. The Zeeman frequency for each solenoid setting was also measured to establish the internal magnetic field values and to determine the shielding factor of each maser's magnetic shields. For each measurement set, the coil was switched a few times before taking data to eliminate transient effects due to slight regaussing of a maser's magnetic shields by the solenoid field. For the one gauss change at the test maser, the field change at the reference maser was only 1.5 mG. This corresponds to less than 10^{-15} frequency shift in the reference maser.

Figure 15 shows the magnetic susceptibility (dy/dH) of NR-1 as a function of Zeeman frequency (Z) for the maser main field coil at minus polarity (arbitrary reference). Notice there are two nulls in dy/dH. One is at Z = 775 Hz. Further data at higher Zeeman frequencies showed dy/dH becoming increasingly negative until it reached a value of -4.9×10^{-13}/G at Z = 13750 Hz, the highest Z at which data was taken.

Figure 16 shows the magnetic susceptibility of NR-1 for the maser main field polarity positive. Notice that only one null in dy/dH appears at the low value of Z, and that around Z = 775 Hz, dy/dH is about 1×10^{-13}/G. Further data shows dy/dH becoming more positive at higher Z until a value of 5.8×10^{-13}/G is reached at Z = 13440 Hz, the highest Z at which data were taken. Over the whole range of Z for which data were taken for both signs of the main field, the change in Z (dZ/dH) remained the same to within ± 1 Hz. Its average value was dZ/dH = 38.9 Hz/G which corresponds to a shield factor (SF) for NR-1 of 3.6×10^4.

Figure 17 shows susceptibility data for NR-2 for its main field positive, notice the zero in dy/dH at Z = 750 Hz. For NR-2's main field, negative dy/dH – 1.8×10^{-15}/G at Z = 769 Hz. The change in sign of the main field from NR-1 to NR-2 for producing the higher field null in dy/dH was caused by inadvertent reversal of the main field coil connections in NR-2. For this data in NR-2,

$$dZ/dH = 60.5(5) \text{ Hz/G}$$

and

$$SF = 2.3 \times 10^4.$$

Notice that the null in dy/dH occurs at approximately the same Z even though there is a large difference in shielding factor between the NR masers.

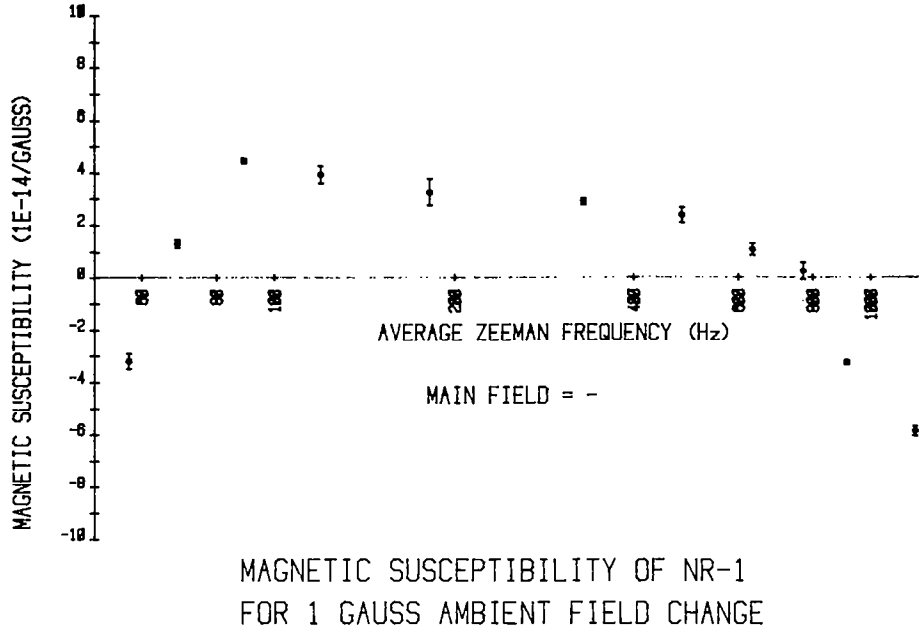

Figure 15. Magnetic susceptibility of NR-1 for main field -.

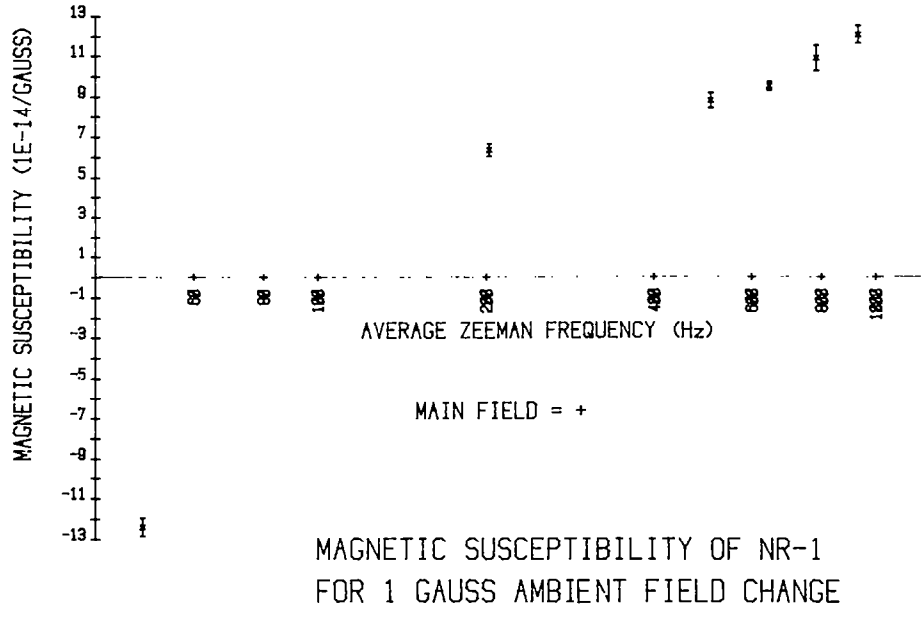

Figure 16. Magnetic susceptibility of NR-1 for main field +.

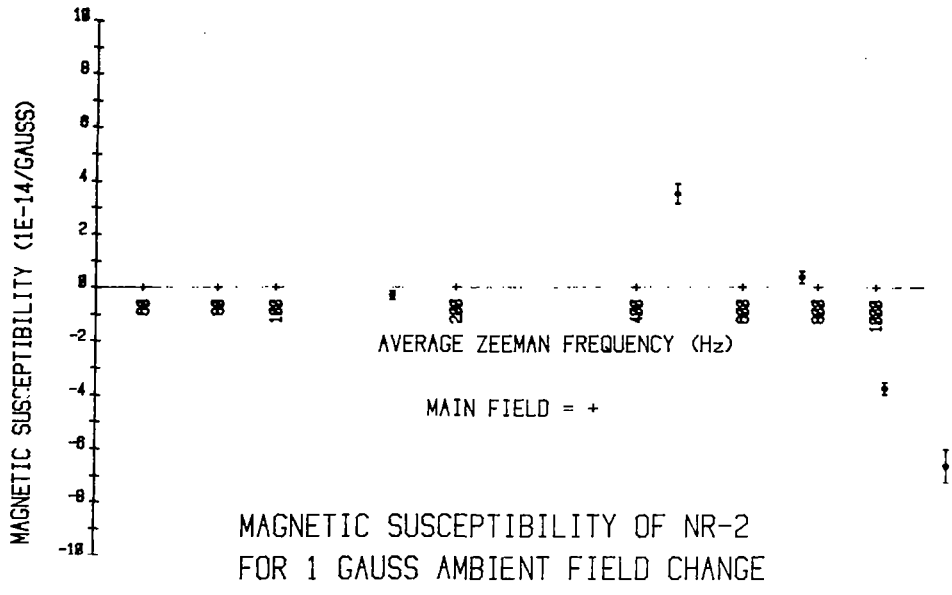

Figure 17. Magnetic susceptibility of NR-2 for main field +.

Figure 18 shows data on the repeatability of the zero susceptibility point at Z = 752 Hz of NR-2. NR-2 was chosen because it has the lower shielding factor. For the first five data points, the standard measurement procedure was used. For the next data points, the solenoid (coil) was changed only once and several frequency measurements were made for each solenoid setting. This was done to check for any systematic errors introduced by the standard measurement procedure and to determine the one time frequency shift caused by regaussing of the maser magnetic shields by the solenoid. Notice that when going from a solenoid field both from 0 to +.5 G and from 0 to -5 G the maser frequency shifted by 1.5×10^{-14}. (The data in the chart are normalized to susceptibility units). Using all susceptibility data except that representing the permanent shifts, one obtains:

$$\text{mean } dy/dH = -0.23 \times 10^{-14}/\text{G}$$

$$\text{standard deviation of points} = 1.08 \times 10^{-14}/\text{G}$$

Thus, NR-2 would be characterized after degaussing as undergoing a one time permanent 1.5×10^{-14} shift from a large magnetic disturbance and then having a susceptibility of about 1×10^{-14}/G for subsequent disturbances.

The data outlined indicates that by finding the zero susceptibility point in each NR maser, one can obtain operational magnetic susceptibilities of 1×10^{-14}/G in these masers. Whether this technique can be applied to hydrogen masers of other designs is another matter since the data presented here may depend on the details of the NR maser design.

	ZEEMAN FREQUENCY (Hz)	SUSCEPTIBILITY (1E-14/GAUSS)
START:	751.8	Ø.17(6)
AFTER MILD MAGNETIC SHOCK:	748.2	1.58(16)
AFTER DEGAUSS:	752.1	-Ø.38(25)
AFTER SEVER MAGNETIC SHOCK & DEGAUSS:	752.7	-Ø.54(68)
AFTER DEGAUSS:	752.5	-1.41(43)
AFTER DEGAUSS & COIL Ø TO -.5 GAUSS:	752.5	-3.21(74)
COIL -.5 TO +.5 GAUSS:	752.5	-1.49(77)
AFTER DEGAUSS & COIL Ø TO +.5 GAUSS:	752.2	2.9Ø(43)
COIL +.5 TO -.5 GAUSS:	752.2	Ø.46(46)

Figure 18. Repeatability of zero susceptibility point of NR-2.

Temperature Sensitivity. The temperature sensitivity of NR-1 was measured. Its value was 4.5×10^{-14} per °C with about a one daytime constant. This is consistent with past measurements on the NX masers which showed a temperature sensitivity of 4×10^{-14} per °C. Because the microprocessor measures the temperature at several points on the maser, this temperature sensitivity can be effectively reduced to zero. Once a maser's temperature coefficient and time constant are measured, the frequency output of the maser can be filtered to extract the predictable temperature shifts. This can be done after the fact by recording temperature changes via the RS-232 interface or in real time by using the RS-232 interface to change the maser synthesizer settings. Though this has not been done yet, such a correction algorithm can be incorporated into the microprocessor programming.

Frequency Stability. Figure 19 shows σ_y (τ) of NR-1 versus NX-2 normalized for one maser. The data are shown both for NR-1's autotuner on and off. This data points out another improvement in the NR masers. The phase shifts which occurred in older Goddard Space Flight Center (GSFC) masers when the flux is changed during autotuning has been reduced to less than one picosecond. As seen from the data, this means that the NR masers can be continuously autotuned with virtually no reduction in their short term stability.

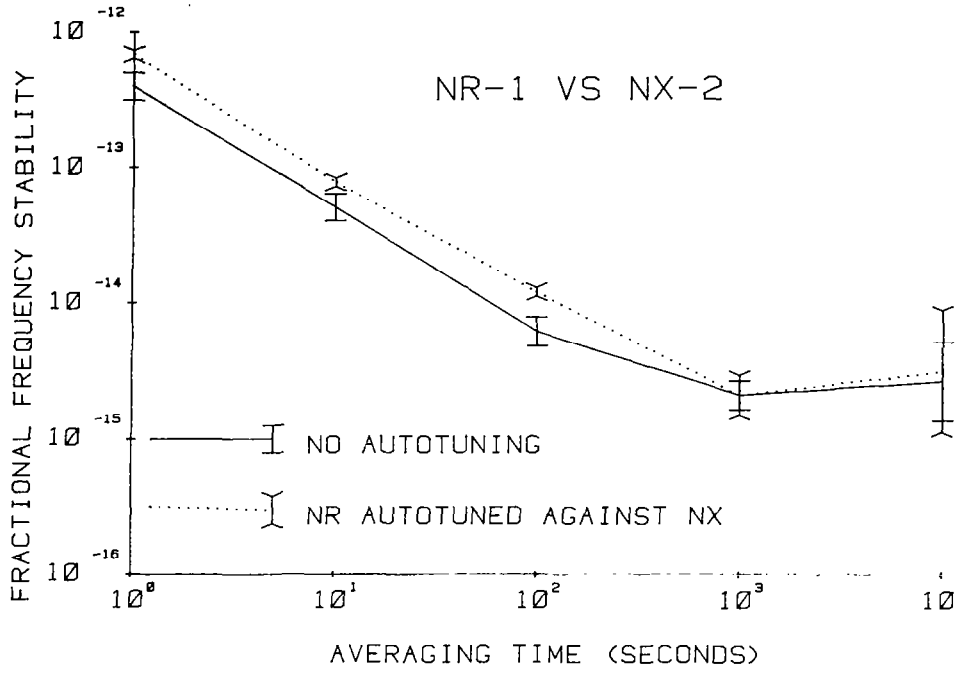

Figure 19. NR-1 stability data.